Characterization of KIF20B as a novel prognostic biomarker and therapeutic target for breast cancer

REGINA WACHUKA MBUGUA[1,2], ATSUSHI TAKANO[1-3], BAYARBAT TSEVEGJAV[1,2], TOMOYUKI YOKOSE[4], TOSHINARI YAMASHITA[5], YOHEI MIYAGI[6] and YATARO DAIGO[1-3]

[1]Department of Medical Oncology and Cancer Center; [2]Center for Advanced Medicine Against Cancer, Shiga University of Medical Science, Otsu, Shiga 520-2192; [3]Center for Antibody and Vaccine Therapy, Research Hospital, Institute of Medical Science Hospital, The University of Tokyo, Tokyo 108-8639; Departments of [4]Pathology and [5]Breast and Endocrine Surgery, Kanagawa Cancer Center; [6]Molecular Pathology and Genetics Division, Kanagawa Cancer Center, Research Institute, Yokohama, Kanagawa 241-8515, Japan

Received October 5, 2023; Accepted January 26, 2024

DOI: 10.3892/ijo.2024.5631

Abstract. Despite advances in treatment and early detection, breast cancer remains one of the most common types of cancer and is the second leading cause of cancer death after lung cancer in women. Therefore, there is an urgent need to develop new biomarkers and therapeutic targets for the treatment of breast cancer. Based on gene expression profiles and subsequent screening performed in a preliminary study, kinesin family member 20B (KIF20B) was selected as a candidate target molecule, because it was highly and frequently expressed in all subtypes of breast cancer and barely detected in normal tissues. Reverse transcription-quantitative PCR and western blotting revealed that KIF20B mRNA and protein expression levels were upregulated in most breast cancer cell lines but were scarcely expressed in normal mammary epithelial cells. Immunohistochemical staining of a tissue microarray showed that KIF20B was detected in 145 out of 251 (57.8%) breast cancer tissues. Strong KIF20B expression was significantly related to advanced pathological N stage. Moreover, patients with breast cancer and strong KIF20B expression exhibited a significantly worse prognosis than those with weak or negative KIF20B expression (P<0.0001, log-rank test). In multivariate analysis, strong expression was an independent prognostic factor for patients with breast cancer. Furthermore, knockdown of KIF20B expression by small interfering RNA inhibited breast cancer cell proliferation and induced apoptosis. In addition, Matrigel cell invasion assays revealed that the invasiveness of breast cancer cells was significantly decreased by KIF20B silencing. Since KIF20B is an oncoprotein that is strongly expressed in highly malignant clinical breast cancer and serves a pivotal role in breast cancer cell proliferation, survival and invasion, KIF20B could be considered a candidate biomarker for prognostic prediction and a potential molecular target for developing new therapeutics, such as small molecule inhibitors, for a wide variety of breast cancers.

Correspondence to: Professor Yataro Daigo, Department of Medical Oncology and Cancer Center, Shiga University of Medical Science, Seta-tsukinowa-cho, Otsu, Shiga 520-2192, Japan
E-mail: ydaigo@belle.shiga-med.ac.jp

Abbreviations: FBS, fetal bovine serum; KIF20B, kinesin family member 20B; HMECs, human mammary epithelial cells; TNBC, triple-negative breast cancer

Key words: KIF20B, breast cancer, biomarker, therapeutic target, oncoantigen

Introduction

Breast cancer remains the most commonly diagnosed type of cancer in women, accounting for one in eight cancer diagnoses globally, with >2,000,000 new breast cancer cases diagnosed and 685,000 breast cancer-associated deaths recorded in 2020 (1). Due to population growth and aging alone, the global burden of breast cancer is expected to increase to >3,000,000 new cases and >1,000,000 deaths by 2040 (2). Notably, there has been a significant decrease in the breast cancer-related death rate over the years, with an overall decline of 43% in 2020 compared with in 1989 (1); however, this decline has slowed slightly in recent years. This decrease has been due to advances in treatment and earlier disease detection through screening. An improved understanding of the biological heterogeneity of breast cancer has also led to advances in the effective and personalized approach of molecular targeted therapies (2).

Based on the expression of hormone receptors (HRs) and growth factor receptors, breast cancer is categorized into distinct molecular subtypes: Luminal A [HR^+ and human epidermal growth factor receptor 2 ($HER2^-$)]; luminal B ($HR^+/HER2^+$); $HER2^+/HR^-$; and triple-negative breast cancer (TNBC; $HR^-/HER2^-$) (3). Globally, of patients with breast cancer, 83% have HR^+ subtypes; of which 71% are luminal A and 12% are luminal B (4). The luminal A subgroup is less

aggressive, more responsive to hormonal interventions and has a better prognosis compared with the luminal B subgroup, which is further defined by its high expression of the proliferation marker antigen Ki67 and $HER2^+$. The $HER2^+$ subtype has high expression of the HER2 oncogene; thus, anti-HER2 therapies may be used for treatment. Globally, the $HER2^+$ subgroup accounts for only 5% of patients with breast cancer, while the remaining 12% of the total patient population has the TNBC subtype (4). Due to the absence of molecular targets, such as overexpression of hormone receptors and HER2, TNBC is more difficult to treat than other subtypes of breast cancer (5).

Clinical classification of breast cancer informs the choice of treatment. In women with advanced or metastatic estrogen receptor $(ER)^+$ and $HER2^-$ breast cancer, palbociclib and abemaciclib were recently approved by the United States Food and Drug Administration for their use in combination with hormone therapy. In addition, alspelisib has been approved as combination therapy with hormonal therapy for the treatment of HR^+ and $HER2^-$ breast cancer with phosphatidylinositol 4,5-bisphosphate 3-kinase catalytic subunit α (*PIK3CA)* gene mutations (6). Trastuzumab and pertuzumab are target therapies selected for the treatment of $HER2^+$ breast cancer. Additionally, trastuzumab has been used in the prevention of relapsed early-stage $HER2^+$ breast cancer. Chemotherapy is the main treatment for TNBC due to its lack of expression of both HRs and HER2; therefore, patients with this type of cancer do not exhibit a response to targeted therapies (7). Pembrolizumab and atezolizumab are some of the immunotherapy drugs recommended for use in patients with metastatic TNBC with tumors expressing programmed death ligand 1 (*PD-L1*). PARP inhibitor drugs, including olaparib and talazoparib, have been used as targeted therapies for TNBC caused by inherited breast cancer gene (*BRCA*) alterations (8).

Several biomarkers for the diagnosis, prognostic prediction and treatment selection of breast cancer have been developed. These include HRs, HER2 and multigene tests, such as Oncotype DX, EndoPredict, MammaPrint and Prosigna (9). Breast cancer biomarkers are constantly evolving from the conventional biomarkers used in immunohistochemistry, such as ER, progesterone receptor (PR) and HER2, to genetic biomarkers with therapeutic implications, such as *BRCA1/2*, *ER*, *HER2*, *PIK3CA* and neurotrophic tyrosine receptor kinase gene mutations, and microsatellite instability (10). Additionally, immunomarkers, such as *PD-L1*, are being employed. While these biomarkers have been developed, they are still limited in their specificity and clinical efficacy (11). Therefore, it is crucial to develop targeted molecular therapies with high accuracy and easily measurable companion diagnostics.

In a preliminary study, target screening for the diagnosis and treatment of cancer was performed by gene expression profile analyses, followed by tissue microarray analyses of solid breast cancer and normal tissues (Fig. S1). Several oncoantigens that were related to carcinogenesis and cancer development have previously been isolated using this screening process (12-32). Following target screening shown in Fig. S1, the present study identified kinesin family member 20B [KIF20B, also known as M-phase phosphoprotein 1 (MPHOSPH1)] as a candidate molecular target that was frequently and highly expressed in breast cancer. KIF20B belongs to the kinesin superfamily, which possesses a highly conserved motor domain, the ATPase activity of which enables it to undergo microtubule-dependent plus-end movement. As a microtubule-associated protein, KIF20B is important for cytokinesis (33). There has been increasing evidence of high expression levels of kinesin family proteins in cancer, suggesting that, in addition to their normal physiological cell function, their upregulation may have oncogenic potential in some types of cancer. Previous reports have suggested that *KIF20B* is highly expressed in some types of human cancer, including hepatocellular carcinoma, bladder, colorectal, pancreatic and tongue cancer (34-38); however, to the best of our knowledge, there has been no detailed investigation on the function of KIF20B in tumorigenesis, and its value as a therapeutic and diagnostic target of various subtypes of breast cancer. This prompted an investigation into the possible role of KIF20B in the development of breast cancer. Therefore, the present study reveals the functional role of KIF20B in breast cancer development, and demonstrates its value as a therapeutic target and prognostic biomarker.

Materials and methods

Breast cancer cell lines and clinical tissue samples. The present study used eight breast cancer cell lines (T-47D, ZR-75-1, MCF7, AU565, SK-BR-3, HCC1599, HCC1937 and MDA-MB-468), which were commercially purchased. Normal primary human mammary epithelial cells (HMECs) were also commercially purchased and the use of primary human cells was approved by the ethics committee. The features of all cells are described in Table I. RPMI-1640 (FUJIFILM Wako Pure Chemical Corporation), EMEM (FUJIFILM Wako Pure Chemical Corporation), McCoy's 5A (Gibco; Thermo Fisher Scientific, Inc.) and Leibovitz's L-15 (Gibco; Thermo Fisher Scientific, Inc.) media supplemented with 10% fetal bovine serum (FBS; Gibco; Thermo Fisher Scientific, Inc.) were prepared and the cells were cultured in monolayers. The cells were incubated at 37˚C in an incubator containing 5% CO_2, with the exception of the MDA-MB-468 cells, which required 0% CO_2 incubation. HMECs were maintained in Mammary Epithelial Cell Basal Medium (cat. no. PCS-600-030) supplemented with Mammary Epithelial Cell Growth Kit (cat. no. PCS-600-040) (both from American Type Culture Collection).

For reverse transcription-quantitative PCR (RT-qPCR), 15 breast tumor samples and three normal breast tissue samples were collected between June 2005 and April 2010 from patients who provided written informed consent at Kanagawa Cancer Center (Yokohama, Japan) (Table SI). The pathologist confirmed that the obtained normal tissues were non-neoplastic and were not contaminated with tumor cells.

The use of the tissues was approved by the Ethics Committee of Kanagawa Cancer Center (approval date: June 8, 2005). In addition, 251 formalin-fixed primary breast cancer tissues and adjacent healthy tissues were obtained from Japanese female patients (median age, 65 years; range, 28-89 years) from Kanagawa Cancer Center for tissue microarray generation. The clinical stage of the breast cancer samples was determined according to the Union for International Cancer Control TNM classification 7th Edition (39). The project to establish tumor tissue microarrays from archival formalin-fixed and paraffin-embedded, surgically obtained tissues and to use

Table I. Human breast cancer cell lines and normal breast cells.

Cell line	Histology	Subtype	Medium	Catalog no.
T-47D	Ductal carcinoma	Luminal A	RPMI-1640	HTB-133
ZR-75-1	Ductal carcinoma	Luminal B	RPMI-1640	CRL-1500
MCF7	Adenocarcinoma	Luminal A	EMEM	HTB-22
AU565	Adenocarcinoma	$HER2^+$	RPMI-1640	CRL-2351
SK-BR-3	Adenocarcinoma	$HER2^+$	McCoy's 5A	HTB-30
HCC1599	Ductal carcinoma	TNBC	RPMI-1640	CRL-2331
HCC1937	Primary ductal carcinoma	TNBC	RPMI-1640	CRL-2336
MDA-MB-468	Adenocarcinoma	TNBC	Leibovitz's L-15	HTB-132
HMECs	Normal breast	N/A	Mammary epithelial cell basal medium	PCS-600-030

Cells were purchased from American Type Culture Collection. TNBC, triple-negative breast cancer; HER2, human epidermal growth factor receptor 2.

the tissue microarrays for later researches was approved by the Kanagawa Cancer Center Ethics Committee (approval no. Rin-177; Yokohama, Japan). The patients whose tissues were used to generate the breast cancer tissue microarrays received surgery at Kanagawa Cancer Center Hospital between January 2004 and March 2006. Written informed consent was obtained from the patients for the use of their clinical information and for specimens remaining after clinical examinations, such as archival formalin-fixed and paraffin-embedded specimens. The ethics committee at Shiga University of Medical Science (approval no. 21-163) approved the present study including the use of all aforementioned clinical materials.

RT-qPCR. Maxwell® 16 LEV simplyRNA Cells and Tissue kits (Promega Corporation) were used to extract total RNA from the cultured cells and clinical tissues according to the manufacturer's protocol. PrimeScript RT Master Mix (Takara Bio, Inc.) was used to synthesize cDNA from total RNA according to the manufacturer's instructions. Samples were incubated at 37˚C for 15 min and 85˚C for 5 sec. mRNA expression was quantified by qPCR analysis using TaqMan® Fast Universal PCR Master Mix (Thermo Fisher Scientific, Inc.) and QuantStudio™ 3 Real-Time PCR System (Applied Biosystems; Thermo Fisher Scientific, Inc.), according to the manufacturer's instructions. For the assays, *KIF20B* (assay ID Hs01027505_m1) primers were used, and β-actin (*ACTB*; assay ID Hs01060665_g1) (both from Thermo Fisher Scientific, Inc.) was used as a control. All experiments were performed in triplicate. The thermal cycling conditions were as follows: Initial denaturation for 20 sec at 95˚C, followed by 40 cycles at 95˚C for 1 sec and 60˚C for 20 sec. Using the $2^{-\Delta\Delta Cq}$ method (40) and with *ACTB* mRNA expression as a reference, *KIF20B* mRNA expression levels were quantified.

Western blot analysis. Cold phosphate-buffered saline (PBS) was used to wash the cells, and RIPA buffer (Pierce; Thermo Fisher Scientific, Inc.) containing a 1% protease inhibitor cocktail was used to lyse the cells. After homogenization, lysates were incubated at 4˚C for 30 min, and the supernatant was centrifuged at 20,400 x g for 15 min at 4˚C to separate proteins from debris. The DC Protein assay kit (Thermo Fisher Scientific, Inc.) was used to measure total protein concentration. A sample buffer containing SDS was then added to the proteins, boiled for 5 min at 100˚C and then incubated at room temperature for 5 min. Using Mini-Protean® TGX 7.5% precast gels (Bio-Rad Laboratories, Inc.), proteins were electrophoresed and transferred onto Trans-Blot® Turbo 0.2 μm polyvinylidene difluoride membranes (cat. no. 1704156; Bio-Rad Laboratories, Inc.). The membranes were blocked in 5% nonfat dried milk in 1X TBS-0.05% Tween 20 (cat. no. 9997; Cell Signaling Technology, Inc.) overnight at 4˚C, after which they were incubated with rabbit polyclonal anti-KIF20B antibody (1:200; cat. no. ab122165; Abcam) or anti-ACTB antibody (1:2,000; cat. no. 12262S; Cell Signaling Technology, Inc.) overnight at 4˚C. Membranes were then incubated with anti-rabbit horseradish peroxidase (HRP)-conjugated secondary antibodies (1:2,000; cat. no. NA934; Cytiva) for 1 h at room temperature. A Fusion Solo S system (Vilber Lourmat) was used to visualize protein bands with chemiluminescence western blotting detection reagents (cat no. RPN2232; Cytiva).

Immunocytochemistry. Cells ($5.0x10^3$ cells/well) were seeded onto an 8-well Lab-Tek II chamber slides (Nalge Nunc International]. The cells were fixed in 4% formaldehyde solution for 15 min at room temperature, washed and then permeabilized using PBS (-) containing 0.2% Triton X-100 for 2 min at room temperature. Thereafter, they were blocked in 3% bovine serum albumin (BSA; FUJIFILM Wako Pure Chemical Corporation) in PBS (-) for 30 min at 4˚C. The cells were then incubated with the rabbit polyclonal anti-KIF20B antibody (1:100; cat. no. ab122165; Abcam) in PBS (-) containing 1% BSA and 0.1% Tween-20 at 4˚C overnight. After washing with PBS (-), the cells were incubated with Alexa Fluor® 488-conjugated goat anti-rabbit IgG secondary antibody (1:800; cat. no. A11008; Thermo Fisher Scientific, Inc.) in a wet chamber for 90 min at room temperature. Nuclei were stained with VECTASHIELD Antifade Mounting Medium containing DAPI (Vector Laboratories, Inc.) and visualized with a confocal laser scanning microscope (Leica TCS SP8 X; Leica Microsystems, Inc.).

Immunohistochemistry and tissue microarray analysis. Tumor tissue microarrays were constructed according to a previously published process (13). Formalin-fixed paraffin-embedded breast cancer tissues and normal tissues were obtained from the Kanagawa Cancer Center. A visually aligned section of hematoxylin- and eosin-stained tissue was used to select the areas for sampling. Slides for tissue microarrays were deparaffinized in xylene and rehydrated in graded concentrations of ethanol. Target Retrieval Solution (pH 9) (Dako; Agilent Technologies, Inc.) was used in a microwave oven for heat-induced antigen retrieval. After blocking endogenous peroxidase activity with a 0.3% hydrogen peroxide/methanol mixture and nonspecific protein binding sites with protein blocking buffer (cat. no. X0909; Dako; Agilent Technologies, Inc.), the sections were incubated with anti-KIF20B antibody (1:200; cat. no. ab122165; Abcam) overnight at 4˚C. After primary antibody incubation, sections were incubated at room temperature for 30 min with polymer anti-rabbit secondary antibodies labeled with EnVision+System-HRP (cat. no. K4003; Dako; Agilent Technologies, Inc.). Specimens were counterstained at room temperature with hematoxylin for 1 min, after being incubated with 3,3'-DAB chromogen and DAB substrate buffer. Since the staining intensity within each tumor tissue core was mostly homogenous, the semi-quantitative evaluation of KIF20B staining intensity was performed by three independent investigators. The expression patterns of KIF20B in tissue arrays were classified from absent/weak to strong. Images of the immunostained samples were acquired with a NanoZoomer whole slide scanner (Hamamatsu Photonics K.K.) and positivity of the KIF20B protein was semi-quantitatively analyzed (30,32) by three independent investigators without prior knowledge of the clinicopathological data. Since the intensity of staining within each tumor tissue core was mostly homogeneous, the staining intensity for KIF20B was recorded as strong positive, weak positive or negative. The staining patterns were defined as strong positive if all of the three reviewers independently classified them as such.

RNA interference assay. To examine the biological functions of KIF20B, small interfering RNAs (siRNAs, 100 μM; Sigma-Aldrich; Merck KGaA) were transfected into T-47D, HCC1937 and SK-BR-3 breast cancer cells ($0.5x10^6$ cells/dish in 10-cm culture dishes) at 37˚C for 5 h using Lipofectamine® 2000 reagent (Invitrogen; Thermo Fisher Scientific, Inc.) according to the manufacturer's instructions. Each gene was targeted using the following sequences: si-KIF20B-#1, sense 5'-GAUGUA UCACUAGACAGUA-3', antisense 5'-UACUGUCUAGUGAUA CAUC-3'; si-KIF20B-#2, sense 5-CAACGAAUUUCAGAA CCUA-3, antisense 5'-UAGGUUCUGAAAUUCGUUG-3'; si-LUC control 1, sense 5'-CGUACGCGGAAUACUUCGA-3', antisense 5'-UCGAAGUAUUCCGCGUACG-3'; and si-EGFP control 2, sense 5'-GAAGCAGCACGACUUCUUC-3', antisense 5'-GAAGAAGUCGUGCUGCUUC-3' (Sigma-Aldrich; Merck KGaA). Western blot analysis was performed 72 h post-transfection, with antibodies against KIF20B to confirm inhibition of KIF20B expression by siRNAs.

For the cell viability assay, breast cancer cells transfected with siRNAs against KIF20B or si-controls were plated in 6-well plates at a density of $0.5x10^5$ cells/well. On day 7 post-transfection, the Cell Counting Kit-8 (CCK-8) solution (Dojindo Laboratories, Inc.) was used to measure cell viability. The cells were incubated with CCK-8 reagent for 4 h and the absorbance was measured at 450 nm using a multi-label plate reader (ARVO X4 system; PerkinElmer, Inc.).

Colony formation assay. A total of $0.5x10^6$ cells/dish were seeded in 10-cm culture dishes and transfected with siRNAs against KIF20B or si-LUC at 37˚C for 5 h. After 7 days, the cells were washed with PBS (-) and fixed with 4% paraformaldehyde phosphate-buffered solution (FUJIFILM Wako Pure Chemical Corporation) at 4˚C for 30 min. The cells were then stained with Giemsa at room temperature for 1 h. A Canon PIXUS-MP990 multifunction device was used to capture the images and colonies, defined as ≥50 cells, were counted.

Annexin V fluorescein isothiocyanate (FITC)-propidium iodide (PI) assay. Breast cancer cells that had been transfected with siRNAs against KIF20B or si-LUC at 37˚C for 5 h were plated in 10-cm dishes at a density of $0.5x10^6$ cells/dish. After 48 h, the cells were trypsinized, washed twice with PBS and then resuspended in 1X binding buffer at a concentration of $1x10^6$ cells/ml. Apoptotic cells were stained using the FITC Annexin V Apoptosis Detection Kit I (BD Pharmingen; BD Biosciences) according to manufacturer's instructions. Control assays were performed to set up compensation and quadrants. The PI-A and Annexin V FITC-A plots were used for gating cells and identifying changes in the scatter properties of the cells. The data were analyzed and the plots were automatically generated using the BD FACSCanto™ II flow cytometer (Ver1.2) and BD FACSDiva™ software (Ver7.0), (BD Biosciences).

Caspase 3/7 expression assay. Caspase 3/7 activities were analyzed using the CellEvent Caspase-3/7 Green Detection Reagent (cat. no. C10423; Invitrogen; Thermo Fisher Scientific, Inc.), according to manufacturer's instructions. Breast cancer cells transfected with si-KIF20B or si-LUC ($0.5x10^6$ cells/dish) were seeded into 6-well plates at a density of $0.5x10^5$ cells/well in an appropriate culture medium containing 10% FBS. The cells were then incubated with CellEvent Caspase-3/7 Green Detection Reagent at a final concentration of 4 μM for 30 min at 37˚C, and then monitored by live cell imaging at 15 min interval for 6 h using the Evos M7000 Auto Imaging System (Thermo Fisher Scientific, Inc.).

Flow cytometric analysis. The BD FACSCanto™ II flow cytometer (Ver1.2), BD FACSDiva™ software (Ver7.0) and the CycleTEST PLUS DNA Reagent Kit (cat. no. 340242), (all BD Biosciences) were used to carry out flow cytometric analysis of cell cycle progression following the manufacturer's instructions. The breast cancer cell lines were transfected with si-KIF20B-#2 or si-LUC siRNA oligonucleotides at 37˚C for 5 h. To assess DNA ploidy, $1x10^6$ cells/ml were harvested 72 h post-transfection. Briefly, 250 μl solution A (trypsin buffer) was added to the cells and incubated at room temperature for 10 min. Subsequently, 200 μl solution B (trypsin inhibitor and RNase buffer) was then added to the cells, gently mixed by tapping the tube and incubated at room temperature for 10 min. After incubation, 200 μl cold solution C (PI staining solution) was added to the cells and incubated in the dark at

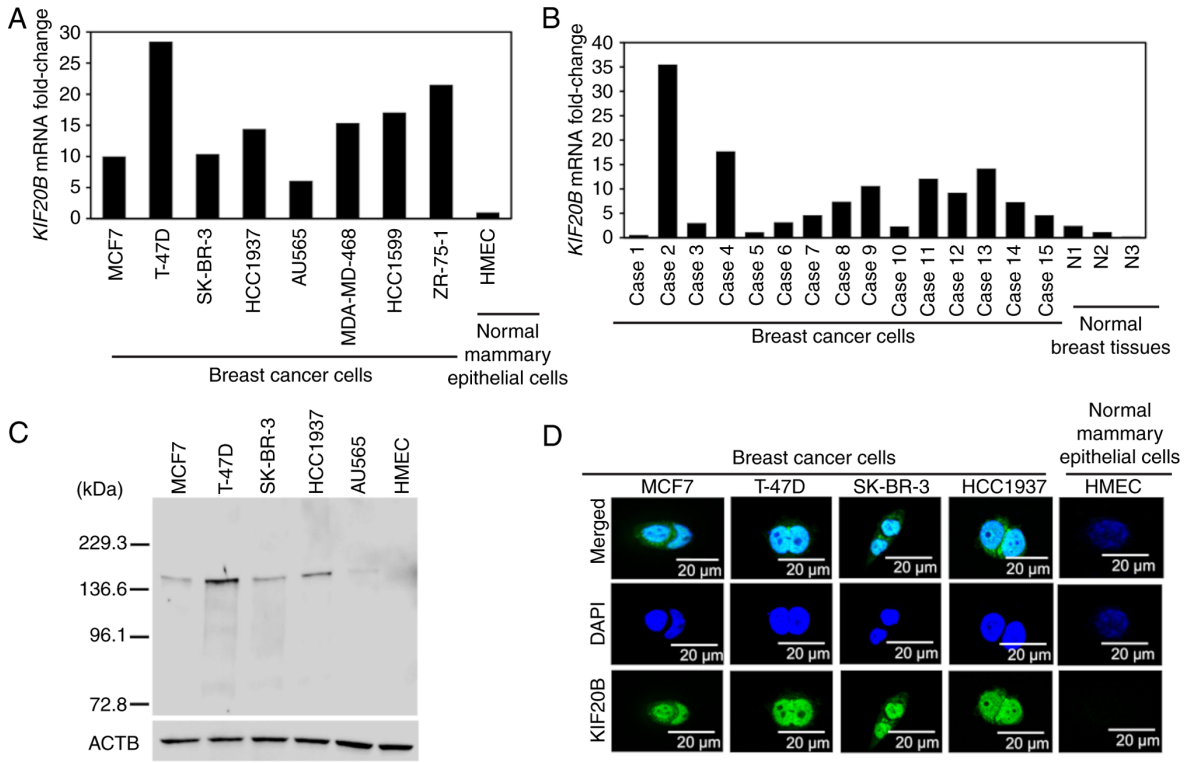

Figure 1. KIF20B expression in breast cancer cells and tissues. *KIF20B* mRNA expression detected using reverse transcription-quantitative PCR in breast cancer (A) cell lines (n=3) and (B) tissues (n=3). The relative fold change in expression in breast cancer cell lines and tissues was compared to those in the normal cell line and tissues, respectively. (C) KIF20B protein expression was detected by western blot analysis in breast cancer cell lines. (D) Subcellular localization of KIF20B protein in breast cancer cell lines and HMECs. Cells were stained with a rabbit polyclonal antibody against KIF20B (green) and DAPI (blue). KIF20B, kinesin family member 20B; HMEC, human mammalian epithelial cells; ACTB, β-actin.

4˚C for 10 min. A 70-μm nylon mesh was used to filter the samples and DNA content was analyzed within 3 h in 20,000 ungated cells.

Live cell imaging. The Evos M7000 Auto Imaging System (Thermo Fisher Scientific, Inc.) was used to monitor cytokinetics. Briefly, breast cancer cells ($0.5x10^6$ cells/dish) transfected with si-KIF20B or si-LUC were seeded into 6-well plates at a density of $0.5x10^5$ cells/well in an appropriate culture medium containing 10% FBS. Cell morphology and dynamics were monitored using the Evos M7000 Auto Cell Imaging System. Images were captured every 15 min over a period of 24 h up to 120 h.

Matrigel invasion assay. Cells transfected with siRNA against KIF20B or with si-LUC were grown to 60% confluence in culture medium containing 10% FBS. After trypsinization, cells were washed with PBS (-) and suspended in medium without serum or protease inhibitor. Matrigel invasion assay was conducted according to the manufacturer's recommendation using Matrigel matrix (BD Biosciences) as described previously (30).

Statistical analysis. Statistical analyses were performed using the Stat View 5.0 Statistical Program (SAS Institute, Inc.). The unpaired Student's t-test was used to analyze the difference between two groups in cell-based assays. Multiple comparisons were conducted using one-way ANOVA followed by Tukey's post hoc test to compare means of each group with those of the other groups. The results are presented as the mean ± standard deviation, and each experiment was performed in triplicate. An analysis of the association between KIF20B expression and clinical variables, including age, histological type, ER, PR and HER2 status, pathological T (pT) and N (pN) stages was conducted using Fisher's exact test. An overall survival (OS) curve was calculated based on the date of surgery and the date of breast cancer-related death or last follow-up. Breast tumors were analyzed for KIF20B expression and Kaplan-Meier curves were calculated for each relevant variable. Log-rank tests were used to analyze differences in survival duration between patient subgroups. To determine whether clinicopathological factors and cancer-related mortality were associated, a Cox proportional hazard regression model was used for univariate and multivariate analyses. In the first step, individual associations between death and possible prognostic factors were examined, including age, ER status, PR status, HER2 status, pT classification and pN classification. Using backward (stepwise) procedures, a multivariate analysis was conducted incorporating KIF20B expression into the model, along with all the variables statistically significant ($P<0.05$) and independent of the other variables. $P<0.05$ was considered to indicate a statistically significant difference.

Database analysis. BioGPS (http://biogps.org/#goto=welcome), GTex Dataset (https://gtexportal.org/home/) and UALCAN (http://ualcan.path.uab.edu/) databases were used to examine the expression of KIF20B in tumor and normal tissues and organs. cBioportal for Cancer Genomics (http://www.

Table II. Association of KIF20B protein expression in breast cancer tissues with patient characteristics (n=251).

Parameter	All patients	Strong positive KIF20B expression	Weak positive KIF20B expression	Negative KIF20B expression	P-value[a]
Total	251	65	80	106	
Age, years					0.2419
<65	188	45	59	84	
≥65	63	20	21	22	
Luminal					0.2687
Positive	177	42	59	76	
Negative	74	23	21	30	
HER2					0.3145
Positive	61	19	22	20	
Negative	190	46	58	86	
pT stage					0.2331
T1-2	86	16	28	42	
T3-4	165	49	52	64	
pN stage					0.0134[b]
N0	142	28	45	69	
N1-2	109	37	35	37	

[a]Strong positive vs. weak positive and negative; [b]P<0.05. KIF20B, kinesin family member 20B; HER2, human epidermal growth factor receptor 2; pT/N, pathological T/N.

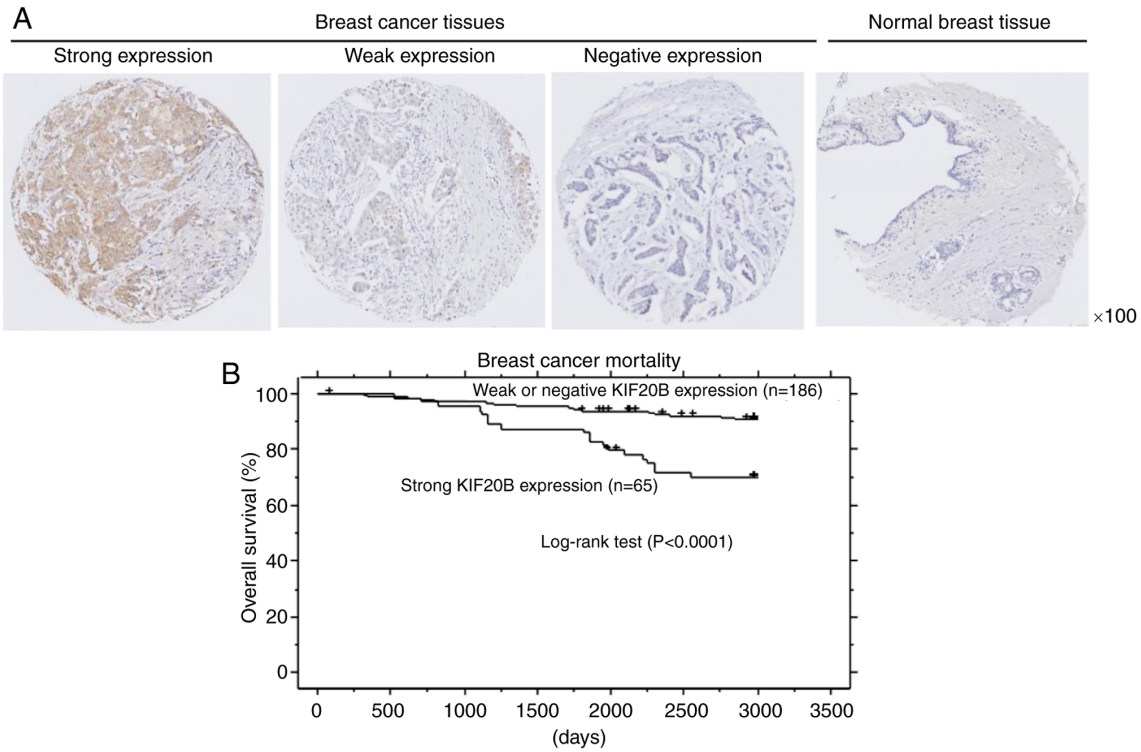

Figure 2. KIF20B expression is associated with poor prognosis in patients with breast cancer. (A) Immunohistochemical staining of KIF20B protein in representative breast cancer tissues. Representative images of strong, weak and absent KIF20B expression, as well as normal breast epithelial tissue are shown (original magnification, x100). (B) Kaplan-Meier analysis of the survival of patients with breast cancer (n=251) according to KIF20B expression (P<0.0001, log-rank test). KIF20B, kinesin family member 20B.

cbioportal.org/) was used to investigate the mutational status of the KIF20B gene. The PrognoScan (http://www.prognoscan.org/) database was used to assess the association between KIF20B expression and the OS of patients with breast cancer.

Table III. Cox's proportional hazards model analysis of prognostic factors in patients with breast cancer.

Variable	Hazard ratio	95% CI	P-value
Univariate analysis			
KIF20B expression (strong positive vs. weak positive and negative)	3.509	1.823-6.755	0.0002[a]
Age (≥65 vs. <65 years)	1.382	0.68-2.808	0.3717
Luminal type (negative vs. positive)	1.834	0.945-3.558	0.0729
HER2 (positive vs. negative)	2.157	0.725-2.997	0.2835
pT stage (T3-4 vs. T1-2)	2.886	1.201-6.936	0.0178[a]
pN stage (N1-2 vs. N0)	5.998	2.627-13.695	<0.0001[a]
Multivariate analysis			
KIF20B expression (strong positive vs. weak positive and negative)	2.674	1.375-5.198	0.0002[a]
pT stage (T3-4 vs. T1-2)	1.76	0.714-4.339	0.2198
pN stage (N1-2 vs. N0)	4.554	1.94-10.69	0.0005[a]

[a]P<0.05. CI, confidence interval; KIF20B, kinesin family member 20B; HER2, human epidermal growth factor receptor 2.

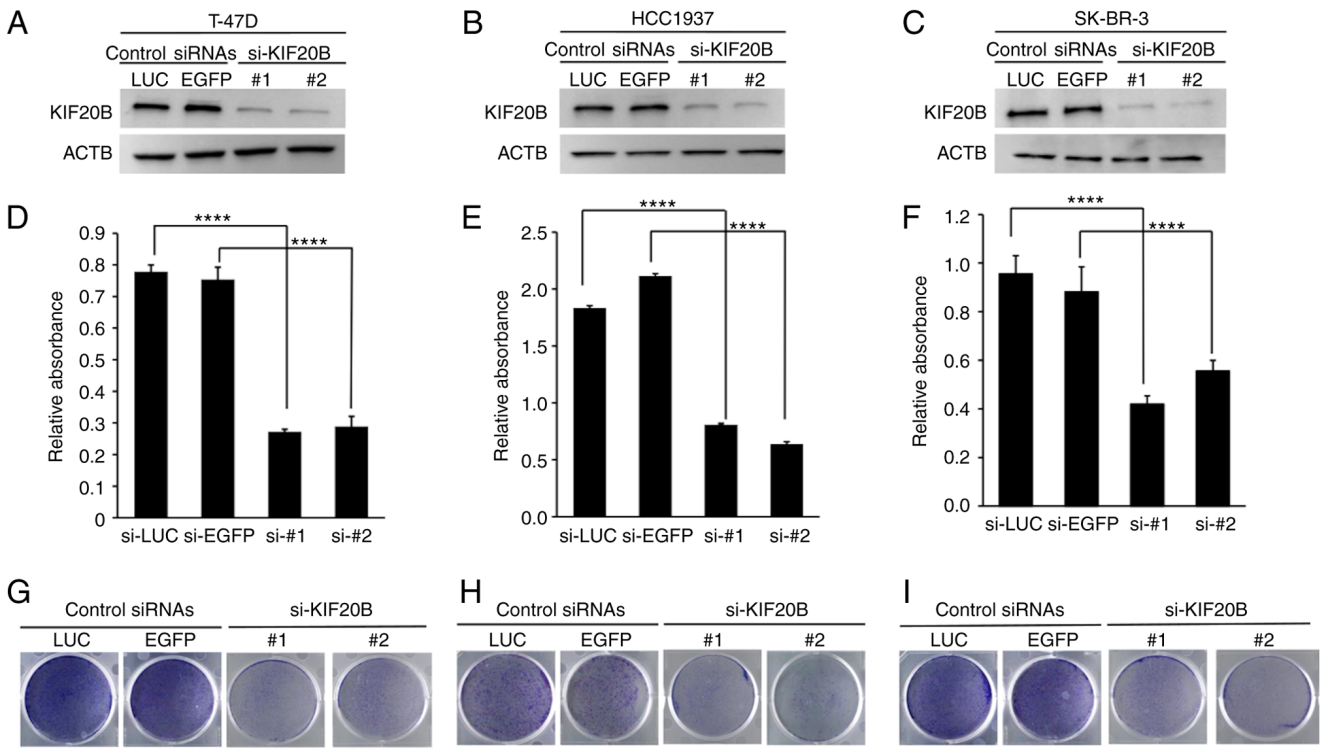

Figure 3. Inhibition of breast cancer cell proliferation by KIF20B knockdown. Suppression of KIF20B protein expression in (A) T-47D, (B) HCC1937 and (C) SK-BR-3 breast cancer cell lines transfected with si-KIF20B and control siRNAs (LUC and EGFP) as determined by western blot analysis. MTT assay was performed to assess the viability of (D) T-47D, (E) HCC1937 and (F) SK-BR-3 cells transfected with si-KIF20B or control siRNAs. Colony formation assay of (G) T-47D, (H) HCC1937 and (I) SK-BR-3 cells transfected with si-KIF20B or control siRNAs. All assays were performed in triplicate (n=3). Data are presented as the mean ± SD. ****P<0.0001. KIF20B, kinesin family member 20B; si, small interfering; ACTB, β-actin.

Results

KIF20B expression in breast cancer cell lines and tissues. Using RT-qPCR, *KIF20B* mRNA expression was detected in all of the breast cancer cell lines and tissues; however, scarce expression was observed in normal breast epithelial cells (HMECs) and tissues (Fig. 1A and B). Cell lines representing each of the three breast cancer subtypes were selected for western blotting and immunocytochemistry experiments in the present study. KIF20B protein was found to be highly expressed in breast cancer cells when compared with HMECs as detected by western blotting (Fig. 1C). Furthermore, immunocytochemical analysis showed that KIF20B protein was mainly localized in the cytoplasm and nuclei of KIF20B-positive breast cancer cells (Fig. 1D).

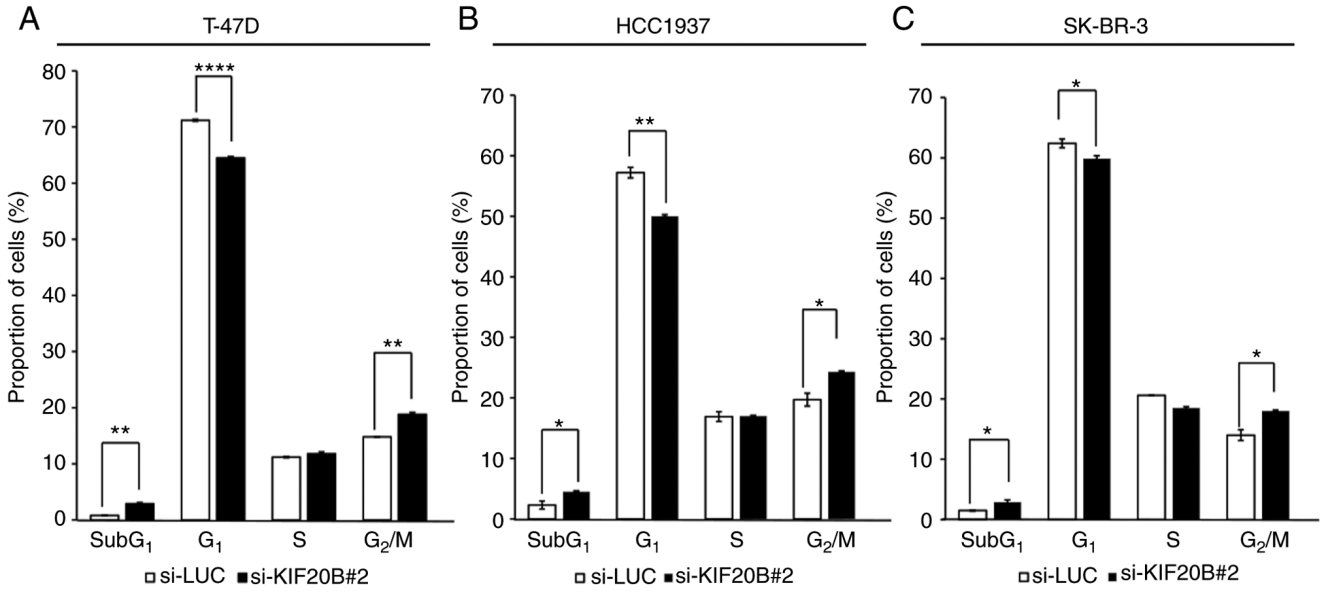

Figure 4. Inhibition of cell cycle progression by KIF20B knockdown. Flow cytometric analysis of cell cycle progression after knockdown of KIF20B by si-KIF20B#2 in (A) T-47D, (B) HCC1937 and (C) SK-BR-3 cells. The assays were performed in triplicate (n=3). Data are presented as the mean ± SD. *P<0.05, **P<0.01, ****P<0.0001. KIF20B, kinesin family member 20B; si, small interfering.

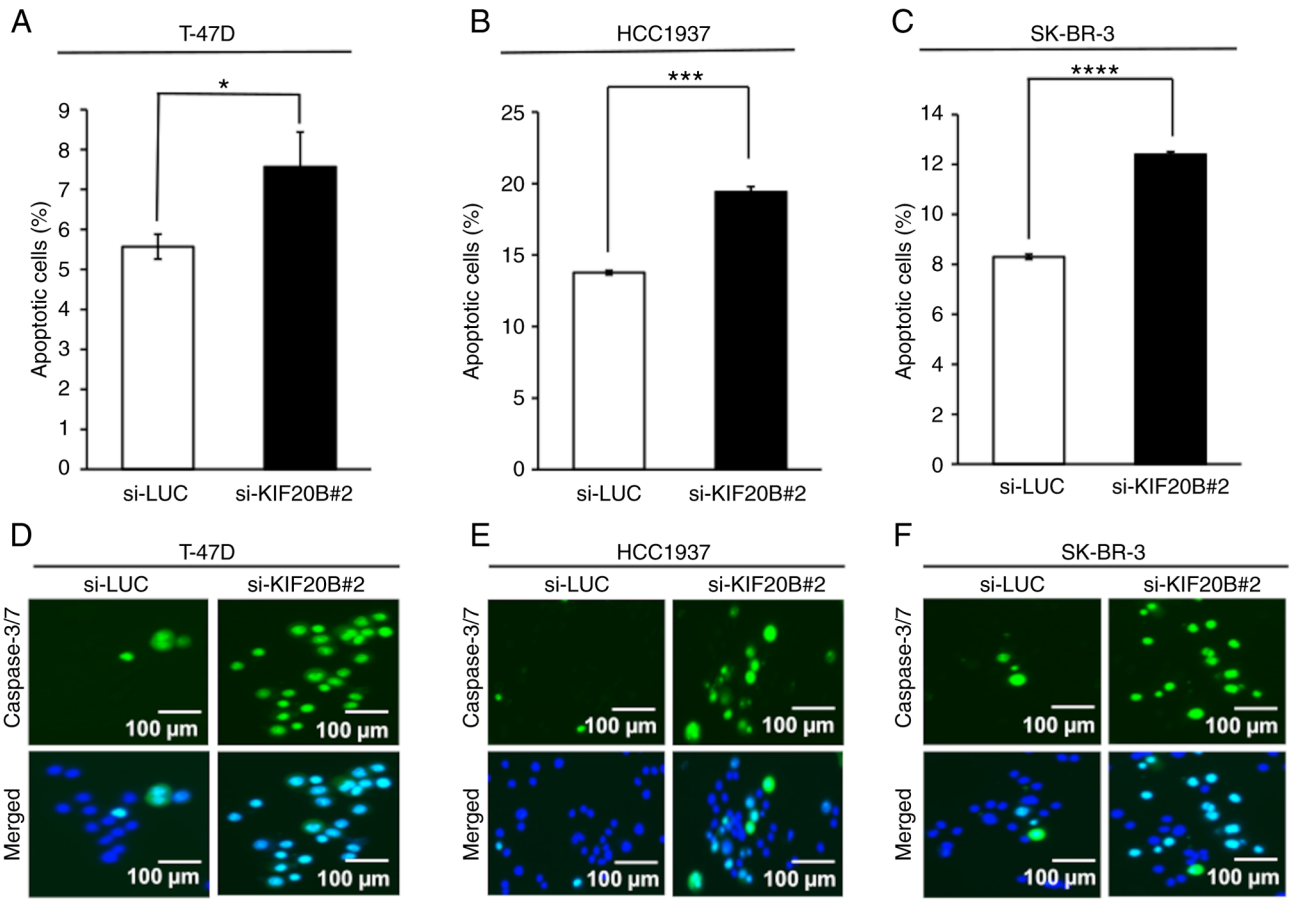

Figure 5. Induction of apoptosis of breast cancer cells by KIF20B knockdown. Percentage of apoptotic (A) T-47D, (B) HCC1937 and (C) SK-BR-3 cells after si-KIF20B#2 or si-control transfection. Detection of apoptotic (D) T-47D, (E) HCC1937 and (F) SK-BR-3 cells after transfection with si-KIF20B#2 or si-control (apoptotic cells are stained with green fluorescence). The assays were performed in triplicate (n=3). Data are presented as the mean ± SD. *P<0.05, ***P<0.001, ****P<0.0001. KIF20B, kinesin family member 20B; si, small interfering.

Association of KIF20B expression with poor prognosis in patients with breast cancer. Immunohistochemical analysis detected KIF20B expression in 145 (57.8%) out of the 251 breast cancer tissues (Fig. 2A and Table II). In addition,

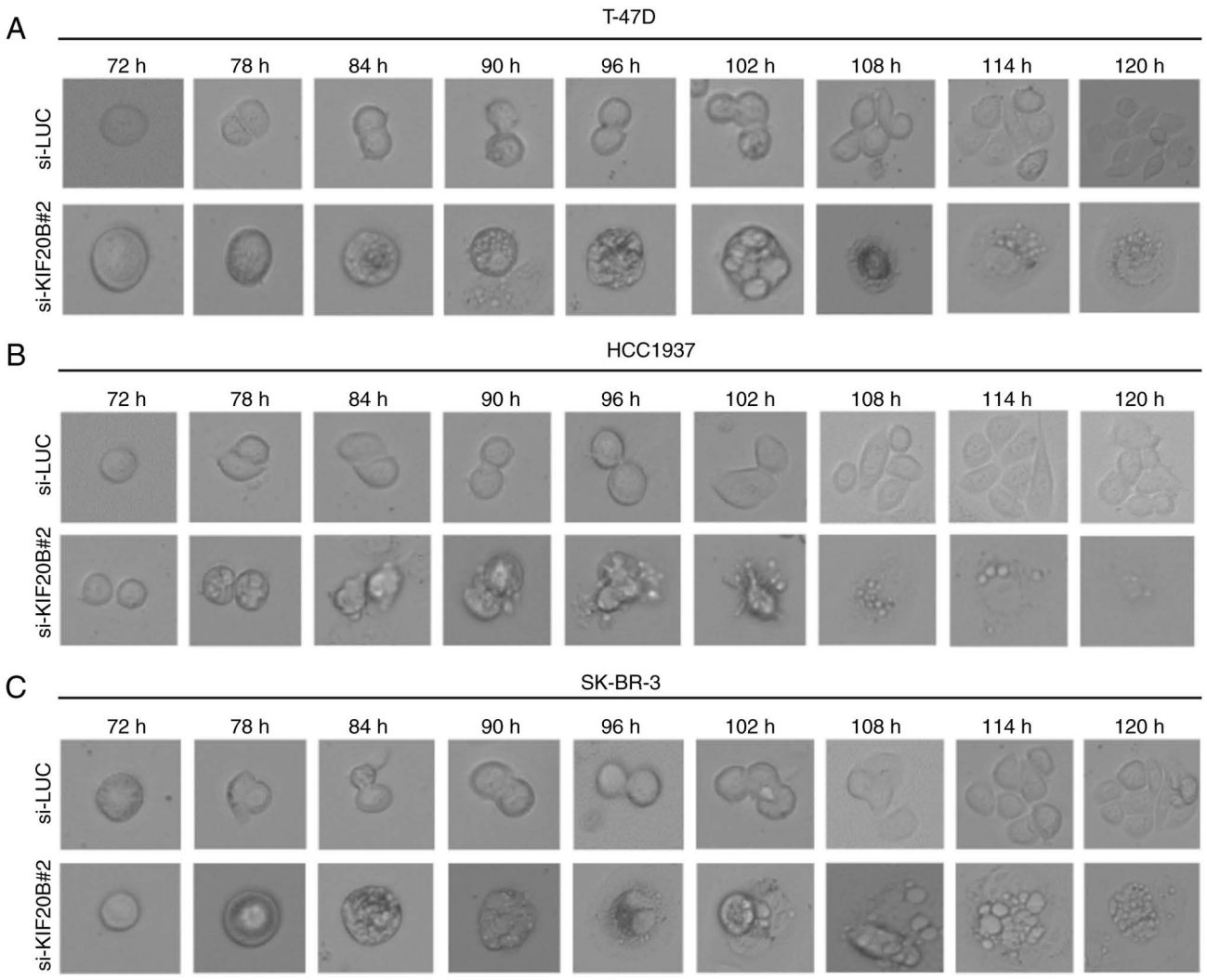

Figure 6. Time-lapse imaging of breast cancer cell dynamics following KIF20B knockdown. Live cell imaging of (A) T-47D, (B) HCC1937 and (C) SK-BR-3 cells transfected with si-KIF20B#2 or control siRNA (magnification, x10) KIF20B, kinesin family member 20B; si, small interfering.

clinicopathological parameters related to KIF20B protein expression were evaluated (Table II). Strong KIF20B expression was significantly related to advanced pN stage. Kaplan-Meier analysis showed that strong KIF20B protein expression was associated with a poorer prognosis in patients with breast cancer (Fig. 2B). Furthermore, univariate analysis was conducted to determine the relationship between patient prognosis and variables, such as KIF20B expression status (strong positive vs. weak positive and negative), age (≥65 vs. <65 years), Luminal type (negative vs. positive), HER2 status (positive vs. negative), pT classification (T3-4 vs. T1-2) and pN classification (N1-2 vs. N0). A strong positive KIF20B expression, an advanced pT stage and an advanced pN stage were significantly associated with a worse prognosis. Furthermore, in multivariate analysis, both strong positive KIF20B expression and advanced pN stage were independent prognostic factors (Table III).

KIF20B knockdown inhibits breast cancer cell proliferation. The expression of KIF20B was suppressed using si-KIF20Bs in T-47D (luminal A), HCC1937 (TNBC) and SK-BR-3 (HER2/neu-positive) breast cancer cell lines. Compared with control siRNAs, si-KIF20B decreased KIF20B protein expression levels in breast cancer cells (Fig. 3A-C). Additionally, MTT assay revealed that si-KIF20B significantly inhibited breast cancer cell viability compared with control siRNAs (Fig. 3D-F). Moreover, colony formation assay showed a marked reduction in breast cancer cell proliferation in response to KIF20B knockdown (Fig. 3G-I).

KIF20B knockdown induces dysregulation of cell division, cell cycle arrest and apoptosis in breast cancer cells. To further examine the mechanism of breast cancer cell proliferation controlled by KIF20B, flow cytometric analysis of cell cycle progression was performed after siRNA transfection. si-LUC was selected for further experiments due to its stability and lower toxicity to breast cancer cells, whereas si-KIF20B-#2 was selected for further experiments because it showed better knockdown effect on KIF20B expression. Compared with si-LUC, at 72 h post-transfection, si-KIF20B#2 significantly increased the proportion of cells at the sub-G_1 and G_2/M phases (Figs. 4A-C and S2). In addition, the number of apoptotic cells was significantly increased after siRNA-mediated KIF20B knockdown compared with that in the control group

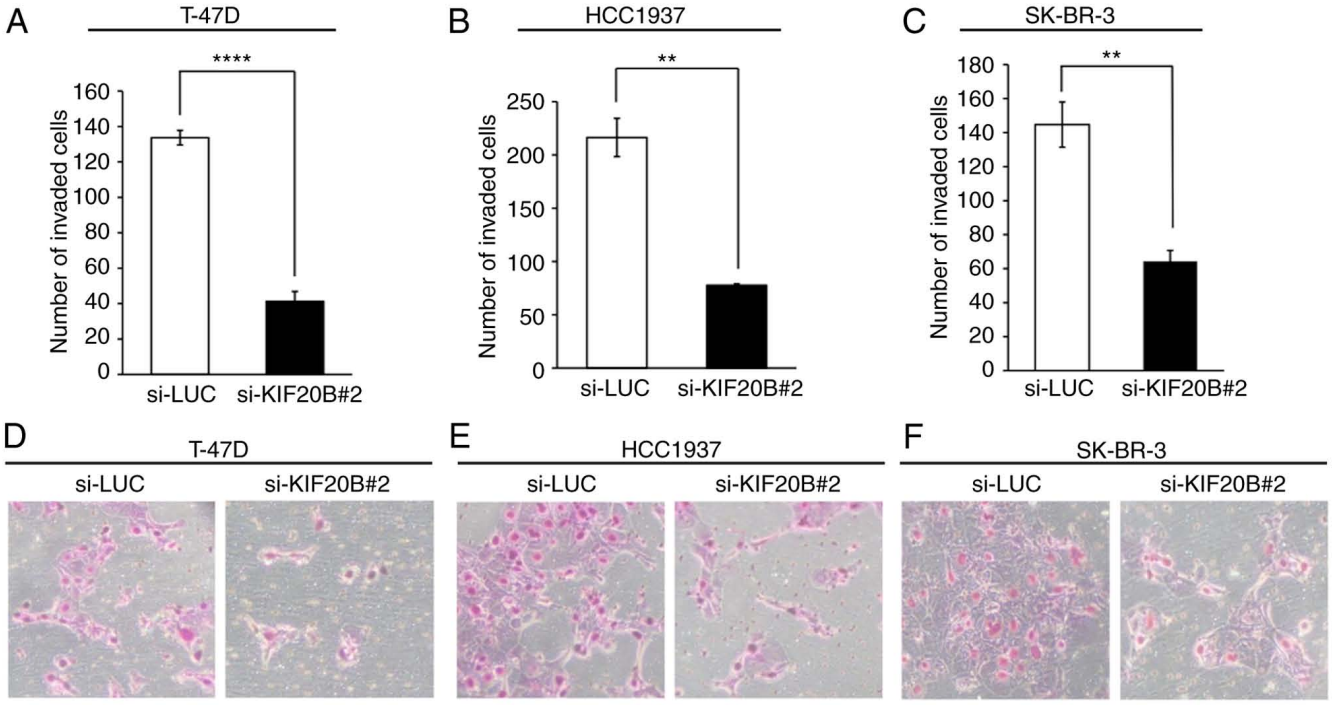

Figure 7. Inhibition of the invasive ability of breast cancer cells by KIF20B knockdown. Relative number of (A) T-47D, (B) HCC1937 and (C) SK-BR-3 cells invading through the Matrigel-coated filters following transfection with si-KIF20B#2 or control siRNA. Giemsa staining of (D) T-47D, (E) HCC1937 and (F) SK-BR-3 invasive breast cancer cells (magnification, x10). Assays were carried out three times and in triplicate wells (n=3). Data are presented as the mean ± SD. **P<0.01, ****P<0.001. KIF20B, kinesin family member 20B; si, small interfering.

(Figs. 5A-C and S3). Additionally, the caspase 3/7 assay demonstrated increased activation of caspase 3/7 in breast cancer cells transfected with si-KIF20B#2 compared with the control siRNA (Fig. 5D-F).

Morphological changes in T-47D, HCC1937 and SK-BR-3 cells transfected with si-KIF20B#2 were further monitored by live cell imaging (Fig. 6A-C). Cells transfected with control siRNAs divided regularly, whereas cells transfected with si-KIF20B#2 did not properly divide and exhibited increased cell death, suggesting that knockdown of KIF20B induces G_2/M arrest and subsequent cell death.

KIF20B knockdown inhibits the invasive phenotype of breast cancer cells. To further elucidate the mechanism underlying the effects of strong KIF20B expression on advanced pN stage, as detected by tissue microarray analysis, Matrigel assays were performed to assess the potential role of KIF20B in the invasion of breast cancer cells. The invasive activity of T-47D, HCC1937 and SK-BR-3 breast cancer cells was significantly reduced after knockdown of KIF20B with si-KIF20B#2 compared with that in the control group (Fig. 7A-F).

Database analysis of KIF20B expression, OS and mutations. In order to validate the expression of *KIF20B* in breast cancer and normal tissues, we examined *KIF20B* data using databases. The BioGPS, GTex Dataset and UALCAN databases showed scarce expression of *KIF20B* gene in normal tissues and organs, and indicated that KIF20B was significantly upregulated in breast cancer tissues compared to normal tissues (data not shown). Using PrognoScan, a significant association between high *KIF20B* expression and reduced OS of patients with breast cancer was identified (dataset no. GSE143; P=0.036199). In order to examine the mechanisms underlying the effects of KIF20B upregulation in breast cancer, KIF20B genetic alterations were investigated using cBioportal for cancer genomics. The genetic aberrations in KIF20B were detected in only 9 of 1,084 breast invasive carcinoma cases (0.83%) (data not shown). Therefore, it was hypothesized that the high expression of KIF20B may be due to several epigenetic mechanisms.

Discussion

Breast cancer is a biologically heterogeneous disease; therefore, the treatment responses and survival outcomes of patients vary. Although significant advances in breast cancer research have been made, it still has high incidence and mortality rates. A wide range of treatments have been developed; however, the OS rates remain low and some subtypes, such as TNBC, are difficult to treat (41). Therefore, the development of new molecular targeted drugs, as well as biomarkers that are novel, precise and cost effective, is desired.

In the present study, KIF20B was found to be highly expressed in breast cancer cells and tissues, but was barely expressed in normal breast epithelial cells and tissues. In addition, knockdown of KIF20B markedly inhibited the proliferation of breast cancer cells and subsequently induced apoptosis. These data suggested the potential of KIF20B as a diagnostic and therapeutic target. Moreover, patients with breast cancer and strong KIF20B expression had a significantly poorer prognosis than those with weak or negative KIF20B expression. The findings from the PrognoScan database independently support the current experimental findings,

indicating that KIF20B might be a prognostic biomarker for breast cancer.

As determined by tissue microarray analysis, strong KIF20B expression was significantly related to advanced pN stage (nodal involvement). Furthermore, the results of a Matrigel cell invasion assay showed that the invasiveness of breast cancer cells was significantly decreased by KIF20B silencing. These data potentially highlight the relevance of KIF20B activation in the malignant potential of breast cancer cells, such as in cell invasion, which is an important factor and the first step in cancer metastasis, a hallmark of malignant tumors, which leads to the dissemination of primary tumor cells to distant organs (42).

KIF20B, a member of the kinesin-6 family, is also known as membrane palmitoylated protein 1 or MPHOSPH1. It is a plus-end-directed kinesin-related protein that serves a crucial role in cytokinesis. In addition, it has been reported to be phosphorylated during the G_2/M transition (43). KIF20B also influences microtubule-binding and microtubule-bundling properties, and microtubule-stimulated adenosine triphosphatase activity *in vitro* (44). Knockdown of KIF20B also potentially induced failed cytokinesis, due to the observed dysregulation of cell division monitored by the live cell imaging and subsequent apoptotic cell death. The present data demonstrated that siRNA-mediated knockdown of KIF20B increased the proportion of breast cancer cells in the sub-G_1 and G_2/M phases. These data independently suggested that KIF20B-mediated cytokinesis and G_2/M transition are important factors in breast cancer cell proliferation and/or survival, and are potential therapeutic targets (Fig. S4). KIF20B is a mitotic target regulated by Pin1, as evidenced by an *in vitro* interaction of the tail domain of KIF20B with the WW domain of Pin1 (45). Pin1 serves an essential role in the regulation of mitosis through its interaction with various mitotic phosphorylated proteins at G_2/M phase transition (46). Furthermore, Pin1 protein is involved in multiple cellular processes, including suppression of apoptosis by directly regulating anti-apoptotic proteins (47). Pin1 has also been reported to be highly expressed in most types of cancer, including human breast cancer (48). These reports indicated the important role of KIF20B in the completion of cytokinesis and that of Pin1 in the regulation of mitosis. In addition, the present data demonstrated the increased proportion of breast cancer cells in the sub-G_1 and G_2/M phases, dysregulation of cell division and subsequent cell death after knockdown of KIF20B. Based on these findings, it was hypothesized that the dysregulation of cell division in KIF20B-depleted breast cancer cells may be caused by mitotic arrest, probably due to failure in cytokinesis, which may lead to errors in chromosomal segregation and subsequent induction of apoptotic cell death. Notably, direct elucidation of the role of KIF20B in cytokinesis, and its relation to microtubules and chromosomal segregation in breast cancer is required. Future studies that examine the potential molecular function of the KIF20B-Pin1 interaction, as well as the oncogenic functions of KIF20B in breast cancer progression, are also warranted.

In conclusion, the findings of the present study suggested that KIF20B is an oncoprotein that serves an essential role in breast cancer cell proliferation and survival, probably through various unknown oncogenic pathways. Notably, KIF20B was also shown to serve a pivotal role in breast cancer cell invasion. Therefore, targeting KIF20B could be an effective approach in the development of new molecular therapies and cancer biomarkers for patients with breast cancer.

Acknowledgements

Not applicable.

Funding

This work was supported in part by a Grant-in-Aid for Scientific Research (B), Grant-in-Aid for Challenging Research (Exploratory), and Grant-in-Aid for Scientific Research on Innovative Areas from the Japan Society for the Promotion of Science (JSPS KAKENHI grant nos. 15H04761, 19H03559, 21K19444, 16H06277, 22H04923 and 23H02815). YD is a member of Shiga Cancer Treatment Project supported by Shiga Prefecture (Japan) and the International Joint Research Project (grant no. FY2016-2024) of the Institute of Medical Sciences (The University of Tokyo).

Availability of data and materials

The data generated in the present study may be requested from the corresponding authors.

Authors' contributions

RWM, AT and YD conceived the research concept and designed the study. RWM, AT and YD developed the study methodology. TYa, TYo, YM and YD acquired the data, managed the patients and provided the facilities. RWM, AT, BT and YD analyzed and interpreted the data (e.g., statistical analysis, biostatistics and computational analysis) and also confirm the accuracy of all the raw data. RWM, AT and YD wrote, reviewed, and/or revised the manuscript. RWM, AT and YD were involved in administrative, technical, and/or material support (i.e., reporting or organizing data, constructing databases). YD supervised the study. All authors read and approved the final manuscript.

Ethics approval and consent to participate

The ethics committee at Kanagawa Cancer Center (approval date: June 8, 2005; approval no. Rin-177) approved the present research and the use of clinical materials. The project to establish tumor tissue microarrays from archival formalin-fixed and paraffin-embedded, surgically obtained tissues and to use the tissue microarrays for later researches was approved by the Kanagawa Cancer Center Ethics Committee (approval no. Rin-177; Yokohama, Japan). Written informed consent was obtained from all patients from Kanagawa Cancer Center for the use of the clinical materials in this study. The ethics committee at Shiga University of Medical Science (approval no. 21-163) approved the present study including the use of all clinical materials.

Patient consent for publication

Not applicable.

Competing interests

The authors declare that they have no competing interests.

References

1. Giaquinto AN, Sung H, Miller KD, Kramer JL, Newman LA, Minihan A, Jemal A and Siegel RL: Breast cancer statistics, 2022. CA Cancer J Clin 72: 524-541, 2022.
2. Arnold M, Morgan E, Rumgay H, Mafra A, Singh D, Laversanne M, Vignat J, Gralow JR, Cardoso F, Siesling S and Soerjomataram I: Current and future burden of breast cancer: Global statistics for 2020 and 2040. Breast 66: 15-23, 2022.
3. Voduc KD, Cheang MCU, Tyldesley S, Gelmon K, Nielsen TO and Kennecke H: Breast cancer subtypes and the risk of local and regional relapse. J Clin Oncol 28: 1684-1691, 2010.
4. Tong CWS, Wu M, Cho WCS and To KKW: Recent advances in the treatment of breast cancer. Front Oncol 8: 227, 2018.
5. Jamdade VS, Sethi N, Mundhe NA, Kumar P, Lahkar M and Sinha N: Therapeutic targets of triple negative breast cancer: A review. Br J Pharmacol 172: 4228-4237, 2015.
6. Raphael A, Salmon-Divon M, Epstein J, Zahavi T, Sonnenblick A and Shachar SS: Alpelisib efficacy in hormone receptor-positive HER2-negative PIK3CA-mutant advanced breast cancer post-everolimus treatment. Genes (Basel) 29: 1763, 2022.
7. Hudis CA and Gianni L: Triple-negative breast cancer: An unmet medical need. Oncologist 16 (Suppl 1): S1-S11, 2011.
8. Robson M, Im SA, Senkus E, Xu B, Domchek SM, Masuda N, Delaloge S, Li W, Tung N, Armstrong A, *et al*: Olaparib for metastatic breast cancer in patients with a germline BRCA mutation. N Engl J Med 377: 523-533, 2017.
9. Hou Y, Peng Y and Li Z: Update on prognostic and predictive biomarkers of breast cancer. Semin Diagn Pathol 39: 322-332, 2022.
10. Chung C, Yeung VTY and Wong KCW: Prognostic and predictive biomarkers with therapeutic targets in breast cancer: A 2022 update on current developments, evidence, and recommendations. J Oncol Pharm Pract 15: 1343-1360, 2023.
11. Ovcaricek T, Takac I and Matos E: Multigene expression signatures in early hormone receptor positive HER 2 negative breast cancer. Radiol Oncol 53: 285-292, 2019.
12. Daigo Y and Nakamura Y: From cancer genomics to thoracic oncology: Discovery of new biomarkers and therapeutic targets for lung and esophageal carcinoma. Gen Thorac Cardiovasc Surg 56: 43-53, 2008.
13. Daigo Y, Takano A, Teramoto K, Chung S and Nakamura Y: A systematic approach to the development of novel therapeutics for lung cancer using genomic analyses. Clin Pharmacol Ther 94: 218-223, 2013.
14. Ishikawa N, Daigo Y, Takano A, Taniwaki M, Kato T, Hayama S, Murakami H, Takeshima Y, Inai K, Nishimura H, *et al*: Increases of amphiregulin and transforming growth factor-alpha in serum as predictors of poor response to gefitinib among patients with advanced non-small cell lung cancers. Cancer Res 65: 9176-9184, 2005.
15. Ishikawa N, Daigo Y, Yasui W, Inai K, Nishimura H, Tsuchiya E, Kohno N and Nakamura Y: ADAM8 as a novel serological and histochemical marker for lung cancer. Clin Cancer Res 10: 8363-8370, 2004.
16. Kakiuchi S, Daigo Y, Ishikawa N, Furukawa C, Tsunoda T, Yano S, Nakagawa K, Tsuruo T, Kohno N, Fukuoka M, *et al*: Prediction of sensitivity of advanced non-small cell lung cancers to gefitinib (Iressa, ZD1839). Hum Mol Genet 13: 3029-3043, 2004.
17. Kato T, Daigo Y, Hayama S, Ishikawa N, Yamabuki T, Ito T, Miyamoto M, Kondo S and Nakamura Y: A novel human tRNA-dihydrouridine synthase involved in pulmonary carcinogenesis. Cancer Res 65: 5638-5646, 2005.
18. Kikuchi T, Daigo Y, Katagiri T, Tsunoda T, Okada K, Kakiuchi S, Zembutsu H, Furukawa Y, Kawamura M, Kobayashi K, *et al*: Expression profiles of non-small cell lung cancers on cDNA microarrays: identification of genes for prediction of lymph-node metastasis and sensitivity to anticancer drugs. Oncogene 22: 2192-2205, 2003.
19. Suzuki C, Daigo Y, Ishikawa N, Kato T, Hayama S, Ito T, Tsuchiya E and Nakamura Y: ANLN plays a critical role in human lung carcinogenesis through the activation of RHOA and by involvement in the phosphoinositide 3-kinase/AKT pathway. Cancer Res 65: 11314-11325, 2005.
20. Kakiuchi S, Daigo Y, Tsunoda T, Yano S, Sone S and Nakamura Y: Genome-wide analysis of organ-preferential metastasis of human small cell lung cancer in mice. Mol Cancer Res 1: 485-499, 2003.
21. Taniwaki M, Daigo Y, Ishikawa N, Takano A, Tsunoda T, Yasui W, Inai K, Kohno N and Nakamura Y: Gene expression profiles of small-cell lung cancers: Molecular signatures of lung cancer. Int J Oncol 29: 567-575, 2006.
22. Oshita H, Nishino R, Takano A, Fujitomo T, Aragaki M, Kato T, Akiyama H, Tsuchiya E, Kohno N, Nakamura Y and Daigo Y: RASEF is a novel diagnostic biomarker and a therapeutic target for lung cancer. Mol Cancer Res 11: 937-951, 2013.
23. Hayama S, Daigo Y, Yamabuki T, Hirata D, Kato T, Miyamoto M, Ito T, Tsuchiya E, Kondo S and Nakamura Y: Phosphorylation and activation of cell division cycle associated 8 by aurora kinase B plays a significant role in human lung carcinogenesis. Cancer Res 67: 4113-4122, 2007.
24. Ishikawa N, Daigo Y, Takano A, Taniwaki M, Kato T, Tanaka S, Yasui W, Takeshima Y, Inai K, Nishimura H, *et al*: Characterization of SEZ6L2 cell-surface protein as a novel prognostic marker for lung cancer. Cancer Sci 97: 737-745, 2006.
25. Kato T, Sato N, Hayama S, Yamabuki T, Ito T, Miyamoto M, Kondo S, Nakamura Y and Daigo Y: Activation of Holliday junction recognizing protein involved in the chromosomal stability and immortality of cancer cells. Cancer Res 67: 8544-8553, 2007.
26. Takano A, Ishikawa N, Nishino R, Masuda K, Yasui W, Inai K, Nishimura H, Ito H, Nakayama H, Miyagi Y, *et al*: Identification of nectin-4 oncoprotein as a diagnostic and therapeutic target for lung cancer. Cancer Res 69: 6694-6703, 2009.
27. Kobayashi Y, Takano A, Miyagi Y, Tsuchiya E, Sonoda H, Shimizu T, Okabe H, Tani T, Fujiyama Y and Daigo Y: Cell division cycle-associated protein 1 overexpression is essential for the malignant potential of colorectal cancers. Int J Oncol 44: 69-77, 2014.
28. Thang PM, Takano A, Yoshitake Y, Shinohara M, Murakami Y and Daigo Y: Cell division cycle associated 1 as a novel prognostic biomarker and therapeutic target for oral cancer. Int J Oncol 49: 1385-1393, 2016.
29. Daigo K, Takano A, Thang PM, Yoshitake Y, Shinohara M, Tohnai I, Murakami Y, Maegawa J and Daigo Y: Characterization of KIF11 as a novel prognostic biomarker and therapeutic target for oral cancer. Int J Oncol 52: 155-165, 2018.
30. Nakamura M, Takano A, Thang PM, Tsevegjav B, Zhu M, Yokose T, Yamashita T, Miyagi Y and Daigo Y: Characterization of KIF20A as a prognostic biomarker and therapeutic target for different subtypes of breast cancer. Int J Oncol 57: 277-288, 2020.
31. Tsevegjav B, Takano A, Zhu M, Yoshitake Y, Shinohara M and Daigo Y: Holliday junction recognition protein as a prognostic biomarker and therapeutic target for oral cancer. Int J Oncol 60: 26, 2022.
32. Zhu M, Takano A, Tsevegjav B, Yoshitake Y, Shinohara M and Daigo Y: Characterization of Opa interacting protein 5 as a new biomarker and therapeutic target for oral cancer. Int J Oncol 60: 27, 2022.
33. Hirokawa N, Noda Y and Okada Y: Kinesin and dynein superfamily proteins in organelle transport and cell division. Curr Opin Cell Biol 10: 60-73, 1998.
34. Kanehira M, Katagiri T, Shimo A, Takata R, Shuin T, Miki T, Fujioka T and Nakamura Y: Oncogenic role of MPHOSPH1, a cancer-testis antigen specific to human bladder cancer. Cancer Res 67: 3276-3285, 2007.
35. Lin WF, Lin XL, Fu SW, Yang L, Tang CT, Gao YJ, Chen HY and Ge ZZ: Pseudopod-associated protein KIF20B promotes Gli1-induced epithelial-mesenchymal transition modulated by pseudopodial actin dynamic in human colorectal cancer. Mol Carcinog 57: 911-925, 2018.
36. Liu X, Zhou Y, Liu X, Peng A, Gong H, Huang L, Ji K, Petersen RB, Zheng L and Huang K: MPHOSPH1: A potential therapeutic target for hepatocellular carcinoma. Cancer Res 74: 6623-6634, 2014.
37. Chen J, Zhao CC, Chen FR, Feng GW, Luo F and Jiang T: KIF20B promotes cell proliferation and may be a potential therapeutic target in pancreatic cancer. J Oncol 2021: 5572402, 2021.
38. Li ZY, Wang ZX and Li CC: Kinesin family member 20B regulates tongue cancer progression by promoting cell proliferation. Mol Med Rep 19: 2202-2210, 2019.

39. Sobin LH, Gospodarowicz MK and Wittekind C (edis): TNM classification of malignant tumours. 7th edition. John Wiley & Sons, 2011.
40. Livak KJ and Schmittgen TD: Analysis of relative gene expression data using real-time quantitative PCR and the 2(-Delta Delta C(T)) method. Methods 25: 402-408, 2001.
41. Cao L and Niu Y: Triple negative breast cancer: Special histological types and emerging therapeutic methods. Cancer Biol Med 17: 293-306, 2020.
42. Pearson GW: Control of invasion by epithelial-to-mesenchymal transition programs during metastasis. J Clin Med 8: 646, 2019.
43. Matsumoto-Taniura N, Pirollet F, Monroe R, Gerace L and Westendorf JM: Identification of novel M phase phosphoproteins by expression cloning. Mol Biol Cell 7: 1455-1469, 1996.
44. Abaza A, Soleilhac JM, Westendorf J, Piel M, Crevel I, Roux A and Pirollet F: M phase phosphoprotein 1 is a human plus-end-directed kinesin-related protein required for cytokinesis. J Biol Chem 278: 27844-27852, 2003.
45. Kamimoto T, Zama T, Aoki R, Muro Y and Hagiwara M: Identification of a novel kinesin-related protein, KRMP1, as a target for mitotic peptidyl-prolyl isomerase Pin1. J Biol Chem 276: 37520-37528, 2001.
46. Cheng CW and Tse E: PIN1 in cell cycle control and cancer. Front Pharmacol 9: 1367, 2018.
47. Liou YC, Zhou XZ and Lu KP: Prolyl isomerase Pin1 as a molecular switch to determine the fate of phosphoproteins. Trends Biochem Sci 36: 501-514, 2011.
48. Wulf GM, Ryo A, Wulf GG, Lee SW, Niu T, Petkova V and Lu KP: Pin1 is overexpressed in breast cancer and cooperates with Ras signaling in increasing the transcriptional activity of c-Jun towards cyclin D1. EMBO J 20: 3459-3472, 2001.